Future Generation of Communication and Internet of Things (FGCIOT)

Journal homepage: http://fgciot.semnaniau.ac.ir/

PAPER TYPE (Research paper)

Stress concentration in the joint of In718 and Mar-M247 superalloys after friction welding using the finite element method

Seyed Rahim kiahosseini[1*]

Department of Mechanical Engineering, Semnan Branch, Islamic Azad University, Semnan, Iran

Article Info

Article History:
Received: 15 October 2024
Revised 14 December 2024
Accepted 27 December 2024

Keywords:
Friction stir welding, superalloy, stress concentration factor, contact in ANSYS

*Corresponding Author's Email Address:
sr.kiahosseini@iau.ac.ir

Abstract

Friction stir welding or FSW is a modern welding method that is performed by creating friction between two parts and generating heat during the welding process. On the other hand, in welded joints, stress concentration will cause a local increase in stress at the weld joint. Also, thermal residual stresses are created in the welding area and its surroundings, which are affected by local heat. The purpose of this research is to model and analyze the friction stir welding butt joint of the nickel-based homonymous superalloys IN718 and the non-homonymous joint IN718 and Mar-M247 using ANSYS software, and then to obtain the stress concentration coefficient of the welded joint of homonymous and non-homonymous superalloys. Finally, the stress concentration coefficients of homonymous and non-homonymous joints were examined together and also compared with experimental data. The results showed that the average stress concentration coefficient in the connection of the same-name superalloys Mar-M247 is 1.566, in the connection of the non-synonymous superalloys IN718 and Mar-M247 it is 1.63, and in the connection of two same-name superalloys IN718 it is 1.52.

Introduction

Superalloys are engineering materials that are widely used at high temperatures due to their unique properties such as strength, creep resistance and hot corrosion [1-3]. In order to use these alloys in industries, it is necessary to create various connections between them. Friction stir welding is one of the new welding methods that was invented by the British Welding Institute with high potential in late 1991 and was registered as a new solid-state welding method[4, 5]. Unlike conventional welding methods that are performed in the molten state, this welding is performed in the solid phase, which was initially used to join non-ferrous metals such as 2xxx series aluminum, but the advancement of welding tools and the manufacture of tools such as B4C, WC and PCBN made it possible to weld materials with high melting points such as various steels or nickel and titanium alloys and other materials with this method[6-9]. Friction stir welding has been considered as the most important development in joining metals in the last decade, which has high energy efficiency and is called green technology due to its energy saving, low pollution and environmental friendliness. This method does not use any shielding gas or flux[10, 11]. It also does not require electrodes or filler materials[12]. On the other hand, some types of discontinuities found in welds include: porosity, incomplete melting, incomplete penetration in the seam, cutting (burning) of the weld edge, overlap, cracks, slag impurities, excess welding dust[13]. For structures that are under fatigue or cyclic load, the risk of these surface discontinuities increases[14]. The presence of geometric discontinuities in the parts causes the stress around the notch to increase sharply locally, hence it is said that there is a stress concentration around the notch[15]. The geometric or

Doi:

elastic stress concentration coefficient is defined as Equation 1[16]:

$$K_t = \frac{\sigma_{\max}}{\sigma_0} \qquad (1)$$

1. In this equation, σ_{max} is the maximum stress at the notch and σ_0 is the nominal stress value. The geometric (elastic) stress concentration coefficient depends on the geometric shape, geometric discontinuity of the part, and the type of loading (axial, bending, torsional), and the stress concentration coefficient can be used to calculate the maximum stress at the notch when the maximum stress is within the elastic limit[17].

In this study, an attempt has been made to investigate the stress concentration resulting from friction stir welding between two superalloys, In718 and Mar-M247, using ANSYS software.

Research Method

The process of performing friction stir welding analysis in ANSYS:

The steps of welding analysis of two alloys In718 and Mar-M247 by friction welding method using ANSYS software are given in the flowchart shown in Figure 1. The specifications used in the finite element model must be determined completely dependent on temperature because mechanical stress and strain at high temperatures are related to temperature. An element must be used in such analyses that has the ability to couple thermal-structural. In creating contact between two materials, temperature is also considered in the degree of freedom of those elements. Figure 2 shows a general diagram of joining two alloys by friction welding.

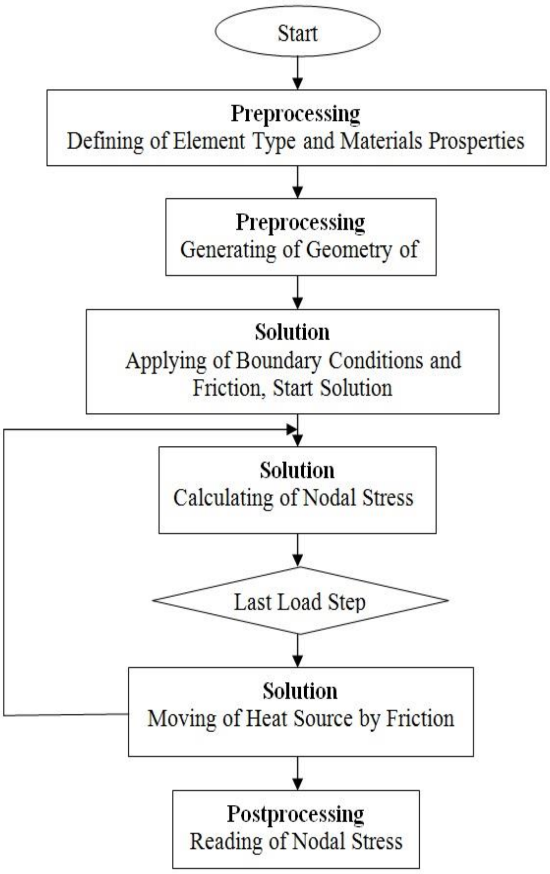

Fig. 1: Flowchart of the analysis process in ANSYS software.

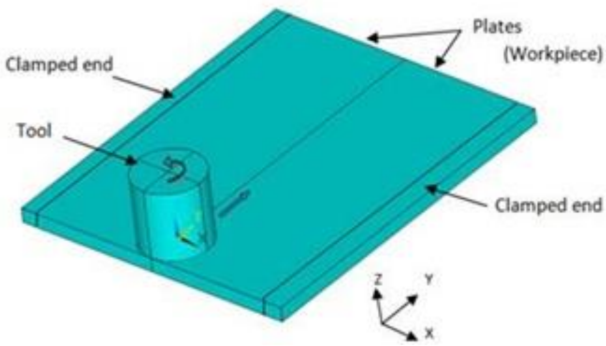

Fig. 2: Geometry of the designed model.

Problem specification:

In this section, the superalloys In718 and Mar-M247 are analyzed by friction welding with a pinless tool. The simulation consists of three stages:

1- Tool engagement with the workpiece.

2- Temperature generation to the welding point by rotating the tool in place on the workpiece.

3- Movement by rotating the tool on the workpiece.

Material specifications of the superalloys:

The chemical compositions of the superalloy IN718 in terms of weight percent are given in Table 1 and the chemical compositions of the superalloy Mar-M247 in terms of weight percent are given in Table 2.

The specifications of the superalloys IN718, Mar-M247 and the specifications of the welding tools are considered in accordance with Table 3.

Table 1: Chemical compositions of IN718[18]

Alloys	C	Si	Cr	Ni	Mo	Fe	Nb	Mn	V	Ti	Al
In718	0.06	0.02	18.55	base	3.02	19.8	4.75	0.05	0.033	0.95	-

Table 2: Chemical composition of Mar-M247[19]

Alloys	C	Ni	Cr	Co	Mo	Fe	Al	B	Ti	Ta	W	Zr	Hf
Mar-M247	0.16	Base	8.2	10	0.6	–	5.5	0.015	1	3	10	0.05	1.5

Table 3: Specifications of IN718, Mar-M247 superalloys and specifications related to welding tools[20-23]

Material properties of the plates (In718)	Young's modulus	**206GPa**					
	Poisson's ratio	**0.29**					
	Coefficient of thermal expansion	**16.9µm/m °C**					
	Yield stress	**861MPa (at 25°C) 1034MPa(at 650°C)**					
	Melting temperature	**1260–1336°C**					
	Ultimate stress	**1275MPa (at 25°C) 1000MPa(at 650°C)**					
	Temperature (°C)	25	200	400	600	800	**1000**
	Thermal Conductivity (W/m °C)	11	12	14	16	17.7	**19**
	Specific Heat (J/Kg °C)	435	455	475	485	495	**510**
	Density (Kg/m^3)	8190	8072	7966	7854	7733	**7594**
Material properties of the plates (Mar-M247)	**Young's modulus**	**199GPa**					
	Poisson's ratio	**0.3**					

	Coefficient of thermal expansion	**18.85µm/m °C**					
	Yield stress	**799MPa (at 25°C) 827MPa(at 650°C)**					
	Melting temperature	**1340 °C**					
	Temperature (°C)	25	200	400	600	800	**1000**
	Thermal Conductivity (W/m °C)	12	13	15	18.9	23	**27.2**
	Specific Heat (J/Kg °C)	300	290	280	300	380	**550**
	Density (Kg/m^3)	8530	8347	8165	8073	7982	**7800**
Material Properties of the PCBN Tool	**Young's modulus**	**680GPa**					
	Poisson's ratio	**0.22**					
	Thermal conductivity	**100 W/m°C**					
	Specific heat	**750 J/Kg°C**					
	Density	**4280Kg/m^3**					

Modeling and Meshing:

In this study, two plates with dimensions of 35*50*70 mm along with a cylindrical tool with a diameter of 30 and a height of 35 mm were assumed using the solid226 element with thermal-structural properties as shown in Figure 3a. Also, the meshed model of the parts in this study is shown in Figure 3b.

According to Figure 3c, surface-to-surface contact targe170 and conta174 with TCC=2e6 w/ m2 °C was used between the two plates. The contact formula type was surface-projection-based contact method and the temperature TBND=1200 was assumed for the connection of the two materials.

According to Figure 3d, the contact between the workpiece and the tool was also made by similar elements, with the difference that the FHTG constant was equal to 1 so that all friction was converted to heat and the FWGT was also set to be equal to 95% so that 95% of the heat was transferred to the workpiece and only 5% of it was transferred to the tool. Also, the value of TCC = 10W/m2 °C is considered very low so that most of the temperature is transferred to the workpiece.

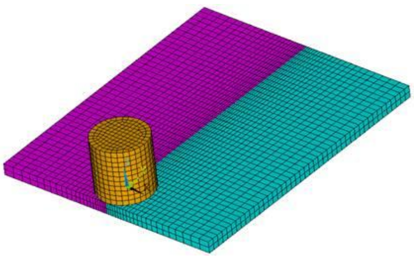

a

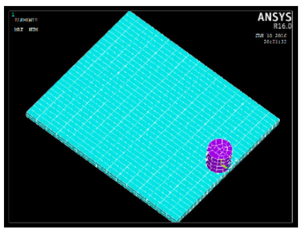

b

c d

Fig. 3: a) Modeled image of the plates and welding pins, b) Meshed model, c) Surface-to-surface contact of targe170 and conta174, and d) Surface-to-surface contact of targe170 and conta174 between the plates and the tool
.

Applying boundary conditions: The boundary conditions were chosen in such a way that the parts were completely constrained on both sides and the following nodes were closed in terms of uz displacement and convection conditions of 30 W/m2 °C were considered at all levels with an initial temperature of 25 °C, but its coefficient at the lower surface of the workpiece was considered to be 10 times that of other surfaces (300 W/m2 °C) and the temperature drop due to radiation was ignored. Then three loading stages were applied as shown in Table 4. The tool enters the workpiece very slightly and starts to rotate. The depth and rotation speed are completely dependent on the welding temperature. The linear speed is considered to be 2.7 mm/s. Then the type of analysis is transition with large deformation and the boundary conditions are applied as linear ramp. The upper limit value of Time step is determined to be 0.2 s due to the type of analysis. In this study, the above-mentioned steps were analyzed once for joining two superalloys of the same name, IN718, and again for joining the superalloy IN718 with the superalloy Mar-M247.

Table 4: Load level and tool rotation and movement parameters[24]

Load Step	Time Period (sec)	Loadings on Pilot Node	Boundary Condition
Penetration	1	Displacement boundary condition	U_Z = -7.95E-07 m
Temperature generation	5.5	Rotational boundary condition	ROT_Z = 60 RPM
Longitudinal movement with rotation	22.5	Displacement and rotational boundary conditions together on the pilot node	U_Y = 60.96E-03 m ROT_Z = 60 RPM

Results and Discussion

The results of modeling and analysis are as follows.

Results of stress level in friction stir welding of superalloys:

First, the penetration of the tool into the workpiece is analyzed by the software. At this stage of the analysis, the tool pin is immersed into the workpiece by a very small amount, which causes a compressive stress in the Z direction, the equivalent von Mises stress at this stage is shown in Figure 4a and b.

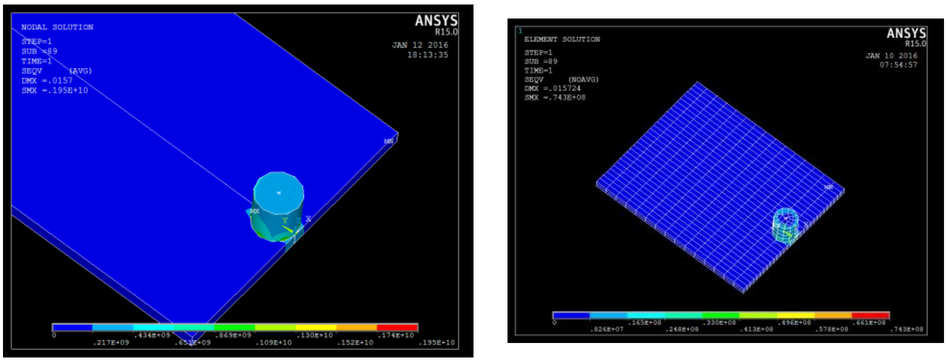

a b

Fig. 4: a) Von Mises stress applied at the end of the tool indentation inside two IN718 pieces, b) Von Mises stress applied at the tool indentation inside IN718 and Mar-M247 .pieces

In the second stage, the pin rotates, which causes frictional stress between the two surfaces and ultimately creates temperature, while the tool penetration remains the same as in the first stage. In this case, the frictional stress causes the workpiece temperature to rise to 70 to 90 percent of its melting temperature and gives the workpiece a paste-like state, which causes friction stir welding of the two pieces butt-to-butt at the beginning of the process. The amount of deformation in the Z direction of the tool during welding is shown in Figure 5.

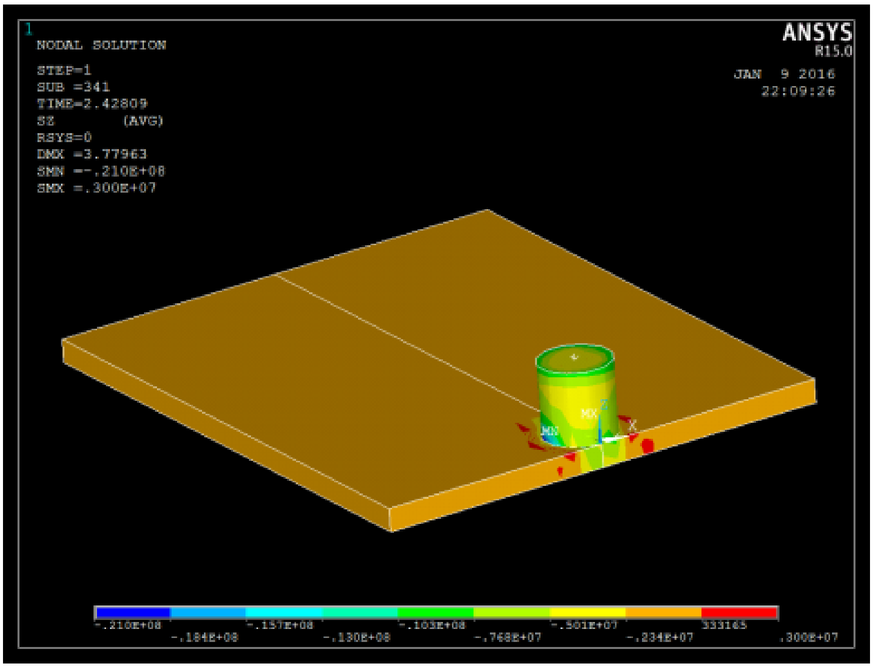

Fig. 5: The amount of deformation in the Z direction of the tool during welding.

In this stage, the maximum stress created by the rotation of the tool pin is transferred to the workpiece, which results in two-surface frictional stress. In the final stage, a linear velocity is given to the tool pin to move along the desired seam along with rotational rotation. As the pin advances, which causes the workpiece to be in a paste state, this paste state continues throughout the weld, causing friction stir welding of the workpiece. The temperature contour at the end of this stage is shown in Figure 6.

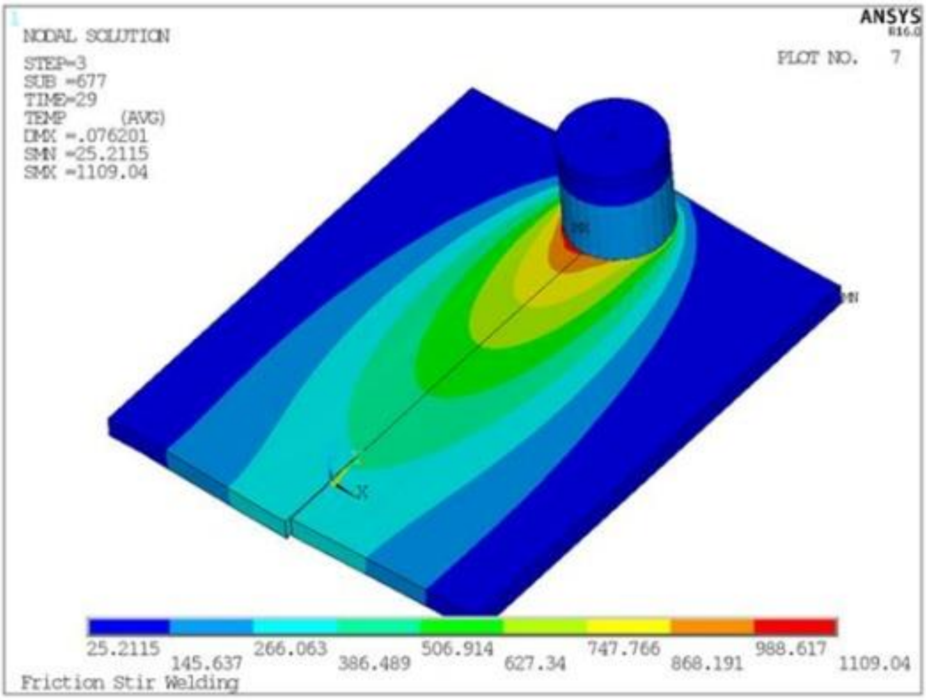

Fig. 6: Temperature contour at the end of friction stir welding.

Verification of friction stir welding by software:

Stress concentration coefficient in the connection of Mar-M247 superalloys by FSW method:

In order to verify the analyses, first we subject the butt friction stir welding performed using ANSYS software to tensile loading. For this purpose, the constraints and loadings related to friction welding analysis are removed from the model and loading is applied in the direction perpendicular to the weld, the results of which are given in Table 5. In this table, the results of friction stir welding of two Mar-M247 alloys are compared with the experimental results extracted from the research of Murray Kaufman[25].

It should be noted that the values of Kt and σ0 are obtained from equation 2, where σ0 is the nominal stress value, F is the tensile force value, h is the thickness (neck) of the weld and l is the weld length[26].

$\sigma_0 = F/hl$ (2)

Table 5: Results of stress concentration coefficient in friction stir welding of superalloys of the same name Mar-M247

Mar-M247 & Mar-M247	**Tensile loading perpendicular to the weld direction**				
F(N)	10 KN	20 KN	30 KN	40 KN	**50 KN**
Tensile stress(Pa)	28.5e+06	57.7e+06	85.6e+06	114.2e+06	**142.8e+06**

Max Tensile stress(Pa)	47.31e+06	86.7e+06	134.3e+06	185+e06	**211e+06**
SCF1	1.66	1.50	1.57	1.62	**1.48**
SCF (Ref value)	1.33	1.33	1.33	1.33	**1.33**
Error (%)	19.8	21.3	15.3	11.3	**10**
(%) Error Avreage			**15.54**		
SCF Avreage			**1.566**		
Error of SCF Avreage & SCF (Ref value) (%)			**15.07**		

Considering the numbers in the table above, it can be seen that the stress concentration coefficient in the connection of two superalloys of the same name Mar-M247 that are connected by friction stir welding is about 1.56, which is 1.33 for a Mar-M247 superalloy, which is an increase in this value considering the friction stir welding process, and the average error percentage in this loading is about 15.07 percent. The existing error percentage shows that the results of the software analysis are in relatively good agreement with the experimental results.

Stress concentration coefficient in joining dissimilar superalloys IN718 and Mar-M247 by FSW method:

To achieve stress concentration in friction stir welding of dissimilar superalloys IN718 and Mar-M247, two welded plates were loaded by the software in the X direction, i.e. perpendicular to the welding direction, and the maximum stress values of the software in the weld section were obtained. The results are shown in Table 6.

Table 6: Results of stress concentration coefficient in friction stir welding of dissimilar superalloys IN718 and Mar-M247

Mar-M247 & IN718	Tensile loading perpendicular to the weld direction				
F(N)	10 KN	20 KN	30 KN	40 KN	50 KN
Tensile stress(Pa)	28.5e+06	57.7e+06	85.6e+06	114.2e+06	142.8e+06
Max Tensile stress(Pa)	47.31e+06	93.47e+06	145.5e+06	177.0+e06	235.6e+06
SCF	1.66	1.62	1.70	1.55	1.65
SCF Avreage			1.63		

Finally, it can be concluded that the stress concentration coefficient in the connection of two superalloys IN718 and Mar-M247, which are connected by friction stir welding, is about 1.63, which is the same value for the superalloys of the same name Mar-M247, which is about 1.56.

Stress concentration coefficient in the connection of two superalloys of the same name IN718 by FSW method:

1 Stress Concentration Factors

The results after loading in the X direction, i.e. perpendicular to the welding direction, were obtained as described in Table 7.

Table (7) Results of the stress concentration coefficient in friction stir welding of superalloys of the same name IN718

IN718 & IN718	**Tensile loading perpendicular to the weld direction**				
F(N)	10 KN	20 KN	30 KN	40 KN	50 KN
Tensile stress(Pa)	28.5e+06	57.7e+06	85.6e+06	114.2e+06	142.8e+06
Max Tensile stress (Pa)	41.8e+06	84.8e+06	124.6e+06	181.5e+06	204.8e+06
SCF	1.61	1.47	1.50	1.59	1.43
SCF Avreage			1.52		

Similarly, it can be said that the stress concentration coefficient in the connection of two superalloys of the same name IN718 that are connected by friction stir welding is about 1.52.

Finally, it can be seen that the stress concentration coefficient in superalloys of the same name IN718 and the same name Mar-M247 is relatively lower than that of non-synonymous superalloys IN718 and Mar-M247.

Regarding friction welding of superalloys of the same name IN718 and the same name Mar-M247, it can be noted that the stress concentration coefficient in Mar-M247 is slightly higher than that in IN718, which is due to the insignificant difference in their mechanical properties. One of these differences is the higher yield stress and modulus of elasticity of superalloy IN718.

Conclusion

The results obtained from this research are as follows:

• In the first stage of friction stir welding, the penetration of the welding pin into the workpiece causes a compressive stress in the Z direction, i.e. perpendicular to the workpiece.

• The rotation of the pin inside the workpiece causes frictional stress in the workpiece, which is at its highest in the Z direction, causes the temperature in the workpiece to increase to about 70 to 90 percent of the melting temperature of the material and gives the workpiece a plastic state.

• Finally, the movement of the pin in the Y direction causes the plastic state of the workpiece to continue throughout the workpiece seam due to the frictional stress resulting from the rotation of the pin and the advancement movement of the pin along the workpiece and connects the two plates.

• In friction stir welding, there is not much difference between the two superalloys of the same name, Mar-M247 and IN718, due to their close mechanical properties.

• The percentage error of the stress concentration coefficient of friction stir welding Mar-M247 with experimental results is about 15.07 percent, which indicates that the software analysis has a relatively good agreement with the reference results.

• The stress concentration coefficient in the existing references for the Mar-M247 superalloy is 1.33, which is obtained in friction stir welding with the software at about 1.56.

• The stress concentration coefficient in the same-name Mar-M247 superalloys is about 1.56 and the same-name IN718 superalloys is about 1.52, which is evident due to the mechanical properties of the yield stress and higher elastic modulus of the IN718 superalloy.

• The stress concentration factor in the superalloys IN718 and Mar-M247 is relatively lower than the non-synonymous superalloys IN718 and Mar-M247, which is about 1.63.

References

[1] Akande, I., et al., Overview of mechanical, microstructural, oxidation properties and high-temperature applications of superalloys. Materials Today: Proceedings, 2021. 43: p. 2222-2231.

[2] Ganji, D.K. and G. Rajyalakshmi, Influence of alloying compositions on the properties of nickel-based superalloys: a review. Recent Advances in Mechanical Engineering: Select Proceedings of NCAME 2019, 2020: p. 537-555.

[3] Simić, M., et al., High temperature materials: properties, demands and applications. Hemijska industrija, 2020. 74(4): p. 273-284.

[4] Akinlabi, E.T. and R.M. Mahamood, Solid-state welding: friction and friction stir welding processes. 2020: Springer.

[5] Li, R. and T. Li, Friction stir welding, in Advanced Welding Methods and Equipment. 2024, Springer. p. 107-146.

[6] Kumar, S. and J.K. Katiyar, Roles of Tribology in Friction Stir Welding and Processing, in Tribology in Sustainable Manufacturing. 2024, CRC Press. p. 162-188.

[7] Bhojak, V., et al., Friction stir process: a comprehensive review on material and methodology. Indian Journal of Engineering and Materials Sciences (IJEMS), 2023. 30(1): p. 45-64.

[8] Kiahosseini, S.R. and A. Aminian, Mechanical and corrosion performance of multilayer ceramic coatings deposited on an austenitic stainless steel using plasma spray. Bulletin of materials science, 2019. 42(4): p. 160.

[9] Kiahosseini, S.R., et al., Adhesion, microstrain, and corrosion behavior of ZrN-coated AZ91 alloy as a function of temperature. Journal of Materials Research, 2013. 28(19): p. 2709-2714.

[10] Arif, M., et al., Green welding. Exploring the environmental and health benefits of friction stir welding over conventional welding methods. Вестник Сибирского государственного индустриального университета, 2023(1 (43)): p. 83-88.

[11] Gajjela, R., et al., Balancing Act Sustainability and Environmental Considerations in Friction Stir Processing of Hybrid Composites. Utilizing Friction Stir Techniques for Composite Hybridization, 2024: p. 316-333.

[12] Raj, A.K., et al. Development of High-performance Welding Consumables and Filler Materials: A Review. in Conference of Innovative Product Design and Intelligent Manufacturing System. 2023. Springer.

[13] Martin, G., et al., WELDING INSPECTION AND NONDESTRUCTIVE EXAMINATION.

[14] Abroug, F., et al., High cycle fatigue strength of additively manufactured AISI 316L Stainless Steel parts joined by laser welding. Engineering Fracture Mechanics, 2022. 275: p. 108865.

[15] Milella, P.P., Notch Effect, in Fatigue and Corrosion in Metals. 2024, Springer. p. 479-518.

[16] Sadat Hosseini, A., M.R. Bahaari, and M. Lesani, Formulas for stress concentration factors in T&Y steel tubular joints stiffened with FRP under bending moments. International Journal of Steel Structures, 2022. 22(5): p. 1408-1432.

[17] Wang, X., S. Li, and L. Peng, A structural curve with reduced stress concentration and its elastic–plastic failure analysis. Engineering Failure Analysis, 2024. 162: p. 108339.

[18] Knorovsky, G., et al., INCONEL 718: A solidification diagram. Metallurgical transactions A, 1989. 20: p. 2149-2158.

[19] Harris, K., G. Erickson, and R. Schwer, MAR-M247 derivations—CM247 LC DS alloy, CMSX single crystal alloys, properties and performance. Superalloys, 1984. 1984: p. 221-230.

[20] Mahaffey, D.W., Inertia Friction Welded Ni-Base Superalloys: Process Examination, Modeling and Microstructure. 2016: The Ohio State University.

[21] Gregori, A. and D. Bertaso, Welding and deposition of nickel superalloys 718, waspaloy and single crystal alloy CMSX-10. Welding in the World, 2007. 51: p. 34-47.

[22] Senkov, O.N., et al., Inertia friction welding of dissimilar superalloys Mar-M247 and LSHR. Metallurgical and materials transactions A, 2014. 45: p. 5545-5561.

[23] Akca, E. and A. Gürsel, A review on superalloys and IN718 nickel-based INCONEL superalloy. Period. Eng. Nat. Sci, 2015. 3(1): p. 15-27.

[24] Liu, D., et al., Finite element analysis of high-speed motorized spindle based on ANSYS. Open Mechanical Engineering Journal, 2011. 5(1): p. 258-67.

[25] Kaufman, M., Properties of cast Mar-M-247 for turbine blisk applications. Superalloys 1984, 1984: p. 43-52.

[26] Shigley, J., C. Mischke, and R. Budynas, Shigley's Mechanical Engineering Design, vol. 8. 2008, McGraw-Hill, New York, NY, USA.